Thiourea and isothiocyanate – two useful chromophores for stereochemical studies. A comparison of experiment and computation†

Jacek Gawronski,* Marcin Kwit and Pawel Skowronek

Received 28th November 2008, Accepted 26th January 2009
First published as an Advance Article on the web 25th February 2009
DOI: 10.1039/b821335f

Thioureas and isothiocyanates, compounds of high importance in organic synthesis, have not been considered so far as chiroptical probes that can provide structural information from the analysis of circular dichroism spectra. CD spectra of a set of molecules containing the thiourea, isothiocyanate and phthalimide chromophores were obtained and analyzed on the grounds of the calculated populations of conformers and their individual contributions to the CD spectra. It is shown that the thiourea and isothiocyanate chromophores can provide useful structural information from the analysis of their exciton-coupled CD spectra. Exciton-coupled CD spectra of thioureas were found to be sensitive to the *Z*/*E* conformation of the chromophore. DFT calculations based on the B2LYP functional were shown to provide a better match with the experimental spectra collected in the short wavelength region, compared to the traditionally used B3LYP functional.

Introduction

Thiourea and isothiocyanates are the two classes of organic sulfur/nitrogen compounds with numerous applications in synthetic organic chemistry, materials chemistry, agriculture[1–3] and crystal engineering.[4] Of particular interest are chiral compounds with thiourea or isothiocyanate functional groups, which may serve as chiral thiourea organocatalysts,[5–12] chiral receptors[13] and chiral derivatizing agents.[14] Despite the wide interest in such molecules, very little is known of their chiroptical properties, electronic circular dichroism (ECD) spectra in particular. Although isothiocyanates and thioureas are derived from amines they have not been considered in the past as useful amine chromophoric derivatives. This is in contrast to other amine chromophoric derivatives, such as Schiff bases, benzamides or aromatic imides,[15–17] which have routinely been used in stereochemical studies.[18] We wish to report that isothiocyanates and thioureas, can serve as useful chromophoric tags, allowing assignment of absolute configuration or conformation from their ECD spectra. We used in this study the derivatives of chiral *trans*-1,2-diaminocyclohexane (DACH) of known conformational rigidity, which allows one to reduce the number of significant conformers and to simplify the calculations of low-energy structures and their ECD spectra. In addition, we used the phthalimide chromophore as a reference for testing exciton coupling power of the isothiocyanate and thiourea electronic transitions. It is known from our previous studies that the principal electronic transition of the phthalimide chromophore is located on its C_2 symmetry axis and therefore its position is insensitive to chromophore rotation.[15]

Many *ab initio* methods are now well established as useful tools for predicting and understanding the chemical and physical phenomena, such as molecular structure, vibronic and electronic spectra with high accuracy.[19] Nowadays there are two different approaches for determination of absolute structure of chiral molecules. X-ray crystallography is successful if a single crystal is available and if the molecule contains at least one heavy atom to allow reliable anomalous dispersion measurements.[20] On the other hand, a comparison of experimental and calculated chiroptical data emerges now as a general and more convenient method,[21] especially in the cases where simple empirical rules for various types of chromophores do not provide correct stereochemical predictions for a broad spectrum of investigated molecules.[22] Among the methods offered currently by theoretical chemistry for stereochemical investigations, those based on time-dependent density functional theory (TDDFT) are most frequently used, and again among the many functionals available, the B3LYP hybrid functional in conjunction with basis sets ranging from the relatively small (*i.e.* 6-31G(d)) to the very large (*i.e.* aug-CC-pVXZ) finds the broadest applicability.[23,24] Although the B3LYP functional is the most frequently used for calculations of many molecular properties, it may not provide satisfactory results for calculations of properties dependent on long- and medium-range noncovalent interactions[25] and for transition metal chemistry. In recent years, the development of new functional forms and their validation against diverse databases have yielded new powerful density functionals of broad applicability to many areas of chemistry.[26] For example, a few years ago Grimme proposed a new functional, containing only two empirical parameters and dubbed B2PLYP,[27] which belongs to a general class of double-hybrid density functionals (DHDFs). This virtual orbital-dependent functional is based on a mixing of standard generalized gradient approximations (GGA) for exchange by Becke (B) and for correlation by Lee, Yang and Parr (LYP) with Hartree–Fock (HF) exchange and a perturbative second-order correlation part (PT2) that is obtained from hybrid-GGA–Kohn–Sham orbitals

---

Department of Chemistry, A. Mickiewicz University, Grunwaldzka 6, 60 780, Poznan, Poland. E-mail: gawronsk@amu.edu.pl; Fax: +48 61 829 1505; Tel: +48 61 829 1313

† Electronic supplementary information (ESI) available: Calculated structures and UV and CD spectra of compounds **1–10**; experimental NMR and MS spectra of compounds **5a**, **5b**, **7**, **8a**, **8b**, **9** and **10**. See DOI: 10.1039/b821335f

and eigenvalues. Several studies have shown that DHDFs give very accurate results for large molecules, thermodynamic data and molecular structures comparable to those from CCSD(T).[28] This and other new functionals are implemented in the latest versions of TURBOMOLE[29] package and they can also be run by Gaussian03[30] ground-state calculations, using the IOPs and extra-overlays given in the original paper.[27] The method was extended recently by Grimme and Neese to electronically excited states in the framework of TDDFT.[31] This procedure is completely analogous with a B2PLYP treatment of the electronic ground state; however, for excited states the corrections to excitation energies are calculated based on configuration interaction with the perturbative double correction method CIS(D).[32] It should be noted that only the energy is corrected in this procedure, while all other computed properties (oscillator and rotatory strengths and transition moments for UV and CD) refer to the TD-hybrid-GGA (in this case TD-B2LYP) level. One should bear in mind, however, that using the IOPs and extra-overlays given in the original paper[27] for excited-state calculations with the use of Gaussian03 package, only the calculations with the hybrid part of the B2PLYP functional can be carried out. For ECD spectroscopy, calculations with the use of DHDFs, including perturbative corrections or not, outperform other TDDFT approaches[33] and therefore can be used as a method of choice for reliable calculations of chiroptical properties of chiral systems.

In this paper we intend to show that thiourea and isothiocyanate molecules can act as chromophores for chiroptical studies. The experimental CD/UV data are analysed on the grounds of TDDFT computational results. We have chosen to use for computations the newly developed functional B2LYP as well as the most popular B3LYP functional for comparison. Due to the size of the molecules used in the present study, we have chosen not to apply the perturbative correction to the excitation energies at the CIS(D) level.

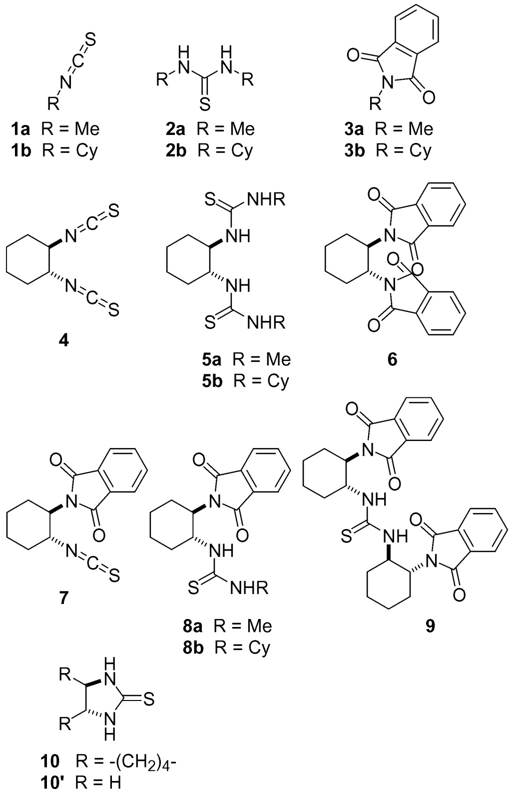

Chart 1

Results and discussion

Synthesis

Cyclohexyl isothiocyanate (**1b**) was commercial and was used without additional purification. Compounds **2b**,[34] **4**,[35] and **6**[15] have been reported in the literature. The synthesis of **5a**, **5b** and **7–10** is quite straightforward and described in the Experimental – it involves the reaction of *N*-phthaloyl-(*R*,*R*)-1,2-diaminocyclohexane[36] with thiophosgene to give **7** or with isothiocyanates **1a** and **1b** to give the thioureas **8a** and **8b**, respectively. The reaction of **7** with *N*-phthaloyl-(*R*,*R*)-1,2-diaminocyclohexane yields symmetrical thiourea **9** while the reaction of (*R*,*R*)-1,2-diaminocyclohexane with thiophosgene yields cyclic thiourea **10** (Chart 1).

Structure

Knowledge of the detailed structure of a molecule is a prerequisite for calculation of its spectroscopic properties. Whereas structures of isothiocyanates and thioureas are deceptively simple, their conformations are not. For the present study we have chosen molecules having different substituents – either small (methyl) or bulky (cyclohexyl) – in order to determine the significance of the steric effects on the conformational equilibria. Both types of molecules were synthesized and characterized by spectroscopic methods as well as by TDDFT calculations of spectroscopic properties.

Our computational studies were performed as follows: (i) conformational searches for simple achiral model molecules **1b**, **2a**, **2b** at the B3LYP/6-311++G(d,p) level, which allowed construction of the PES for these molecules; (ii) full structure optimizations at the B3LYP/6-311++G(2d,2p) level were performed for the energy minima found on the PES; (iii) the results obtained for model compounds were used as input parameters in conformational analyses of more complex molecules **4–9**; (iv) full structure optimizations at the B3LYP/6-311++G(2d,2p) level were performed for low-energy conformations of **4–9**; (v) oscillator and rotatory strengths for thermally accessible conformers of **1–10** were calculated; (vi) for all optimized structures, frequency calculations were carried out at the B3LYP/6-311++G(2d,2p) level of theory to confirm that the conformers are stable; (vii) for the conformers having relative energies ranging from 0.0 to 2.0 kcal mol^{-1}, percentage populations were calculated on the basis of the ΔG values, using Boltzmann statistics and $T = 298$ K.

The results of our DFT calculations at the B3LYP/6-311+G(2d,2p) level for molecules **1–10** are collected in Table 1 (see also Fig. A–C, ESI†).

Methyl isothiocyanate (**1a**) has only one significant planar structure (apart from rotamers due to the methyl substituent), having the calculated C–N=C angle 149.2°. Cyclohexyl isothiocyanate molecule (**1b**) shows a more diverse conformational profile (Fig. 1). Although the equatorial conformer with C_S symmetry and torsion angle α (H–C–N=C) equal to 180° is calculated as a

Table 1 Structures of thermally accessible conformers of **2b**, **4–10** calculated at the B3LYP/6-311++G(2d,2p) level, their relative energies (ΔG) and populations

Compound	Symmetry	ΔG/kcal mol^{-1}	Population (%)	Torsion angles α, α' (°)
2b *Z*,*Z*	C_2	0.00	71	-30^a
2b *E*,*Z*	C_1	0.51	29	-35^a, -30^a
4 *sp*,*sc* (dieq.)	C_1	0.0–0.6	56	$29–34^b$, $40–48^b$
4 *sp*,*sc* (dieq.)	C_1	0.8–1.1	22	$5–48^b$, $-16–91^b$
4 *sc*,*ap* (dieq.)	C_1	0.8	6	54^b, 177^b
4 *sc*,*sc* (dieq.)	C_2	1.0–1.1	8	56^b
4 *ap*,*ap* (dieq.)	C_2	1.5	2	170^b
4 *sc*,*sc* (diax.)	C_1	1.1–1.6	5	$46–64^b$, $60–65^b$
4 *ap*,*ap* (diax.)	C_2	1.9	1	180^b
5a Z^d,Z^d,E,E	C_2	0.00	39	-16^b
5a Z^d,Z^d,Z,Z	C_2	0.11	33	-22^b
5a Z^d,Z^d,Z,E	C_1	0.19	28	-24^b, -15^b
5b Z^d,Z^d,E,E	C_2	0.00	55	40^a, -18^b
5b Z^d,Z^d,Z, E	C_1	0.25	35	-27^a, -9^b, -25^b, 40^a
5b Z^d,Z^d,Z,Z	C_2	0.98	10	-30^a, -18^b
6	C_2	—	>99	4^c
7	C_1	—	>99	62^b, 5^c
8a Z^d,E	C_1	0.00	37	30^b, -18^c
8a Z^d,Z	C_1	0.05	34	32^b, -19^c
8a E^d,Z	C_1	0.12	29	14^b, 13^c
8b Z^d,Z	C_1	0.00	76	30^a, 32^b, -19^c
8b E^d,Z	C_1	0.68	24	-28^a, 18^b, 14^c
9 *E*,*Z*	C_1	0.00	94	-7^c, 40^b, 38^b, -20^c
9 *Z*,*Z*	C_2	1.63	6	32^b, -20^c
10	C_2	—	>99	-81^b

[a] H–$C_{cyclohexane}$–N–C(=S). [b] H–C_{DACH}–N–C(=S). [c] H–C_{DACH}–N–C(=O). [d] C_{DACH}–N–C=S.

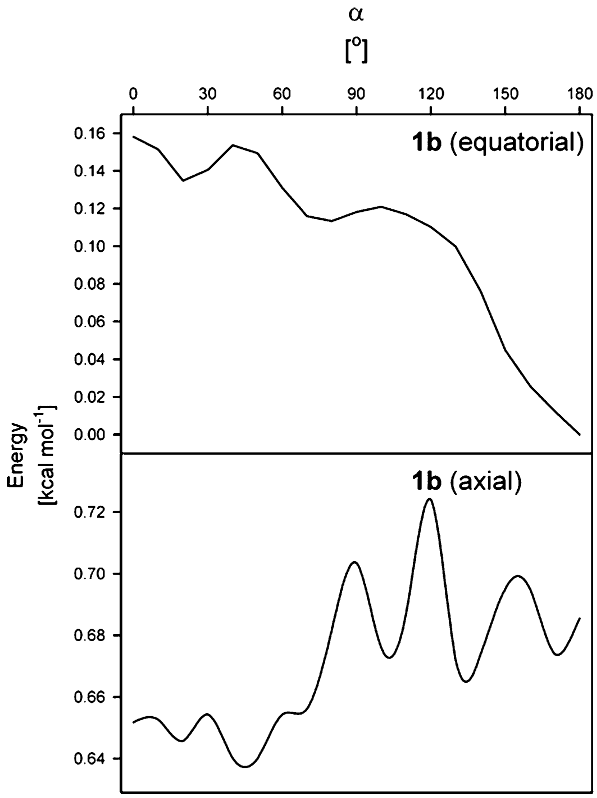

Fig. 1 PES for equatorial and axial conformers of **1b** calculated at the B3LYP/6-311++G(d,p) level.

low-energy structure, rotation of the isothiocyanate group around the C–N bond does not significantly increase the total energy of the molecule. In fact, single-point optimization of geometry of conformer C_S of **1b** leads to the lowest energy structure C_1, having torsion angle $\alpha = 60°$.

Axial conformers of **1b** are generally of higher energy (0.6–0.7 kcal mol^{-1}) compared to the lowest-energy equatorial conformer, and the computation shows again a continuum of accessible conformers of C_1 and C_S symmetry due to the rotation around the C–N bond (Fig. 1).

The conformations of thioureas were previously the subject of study by NMR, IR and X-ray diffraction methods. Three distinct conformers, *Z*,*Z* (*trans*,*trans*), *Z*,*E* (*trans*,*cis*) and *E*,*E* (*cis*,*cis*) can be envisaged, as shown for *N*,*N*′-dicyclohexylthiourea (**2b**) (Fig. 2).

In solution the presence of planar and non-planar conformers is suggested, according to NMR and IR spectra, the *Z*,*E* conformer being the main constituent of the equilibrium mixture.[34,37,38] The conformational equilibria depend on the size of thiourea substituents – planarity of the thiourea molecule is apparently more pronounced for the dimethyl derivative than for other *N*,*N*′-disubstituted derivatives. In the solid state, X-ray diffraction studies show[39] that both low-energy types of conformers, *Z*,*Z* and *Z*,*E*, can be encountered, each conformer type involved in a different pattern of intermolecular hydrogen bonding.[40]

N,*N*′-Dimethylthiourea (**2a**) has two low-energy conformers, *Z*,*E* (planar, C_S symmetry) and *Z*,*Z* (slightly twisted, H–N–C=S angle α = 177°, C_2 symmetry), in an equilibrium ratio 93 : 7. This is in keeping with a general tendency for conformational preferences of dialkyl thioureas and with the results of recent DFT calculations at the B3LYP/6-31G(d) level of the relative energies of conformers of *N*,*N*′-dialkylthioureas.[41] A much higher relative energy has been calculated for the planar *E*,*E* conformer of **2a** as well as for non-planar conformers of **2a** ($0 < \alpha, \alpha' < 180$), in

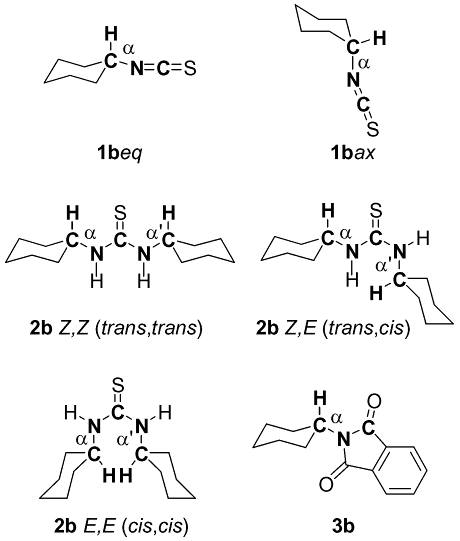

Fig. 2 Definition of torsion angles α in basic conformers of compounds **1b**–**3b**: **1b**, α = H–C–N=C; **2b**, α, α' = H–C–N–C; **3b**, α = H–C–N–C.

comparison to the energies of planar *Z*,*Z* and *Z*,*E* conformers (see Fig. 3).

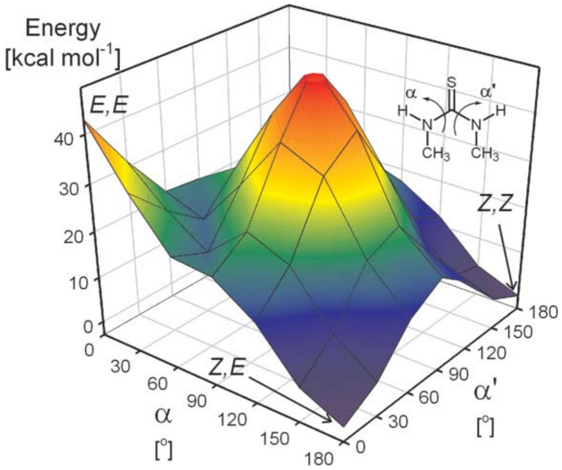

Fig. 3 PES for **2a** as a function of torsion angles α and α' (H–N–C=S) calculated at the B3LYP/6-311++G(d,p) level.

For *N*,*N*′-dicyclohexylthiourea (**2b**), the calculation indicates two thermally accessible conformers, *Z*,*Z* and *Z*,*E*, participating in the equilibrium in the ratio 71 : 29. These conformers are accordingly of C_2 and C_1 symmetry (see Table 1), with torsion angles α *ca.* –30°. Note that in the crystal structure of **2b** the *Z*,*E* conformer shows disorder due to rotation of one of the cyclohexyl groups around the C–N bond.[39a]

Whereas the structure of *N*-methylphthalimide (**3a**) does not require a detailed conformational analysis, the calculated lowest energy structure of the *N*-cyclohexyl analogue (**3b**) was found to have C_S symmetry, conforming to the previously established preference for equatorial phthalimide substituent with the carbonyl group eclipsing the (N)–C–H bond.[15] Diisothiocyanate **4** is of special interest since a rather complex conformational equilibrium can be anticipated due to the small energy differences calculated for the conformers of a related model compound **1b**. To find the relationship between the total energy of the molecule and the rotation of the isothiocyanate substituents, torsion angles H–C*–N–C were changed at 30° steps to give 144 different structures for each diequatorial and diaxial conformers of **4**. Then single-point energy calculations were performed for each conformer and this allowed the construction of the PES for **4** (see Fig. D, ESI). The conformers which were found as the energy minima on the PES were fully optimized at the B3LYP/6-311++G(2d,2p) level of theory. As expected, in all conformers of **4** the isothiocyanate moieties were bent, with the calculated C–N=C angle in a narrow range, 145–147°. The lowest-energy conformers of both diequatorial and diaxial **4** are of C_1 symmetry (Table 1) and are grouped into families of conformers according to the magnitudes of the H–C_{DACH}–N–C(=S) torsion angles. In the family of C_1 symmetry conformers one of the torsion angles is *sc*; bis-*sc* structures are of the lowest energy among the diaxial conformers of **4**. Bis-*ap* structures are of C_2 symmetry and are of higher energy, hence their calculated population is only within 1–2%. The most stable conformers of **4**, diequatorial *sp*,*sc*, count for 78% of the entire conformer population. This is of importance with respect to the discussion of the chiroptical properties of **4** (see below). Note that torsion angles α and α' for conformers of **4** are positive in the majority of cases.

Low-energy structures of dithioureas **5a** and **5b** are uniform in their tendency for *Z* configuration around the C_{DACH}–N–X=S bond (Table 1). They also show a preference toward mixed *Z*/*E* configuration around each thiourea moiety, although all-*Z* and mixed *Z*,*E*/*Z*,*Z* structures do not differ much in their energies, except the all-*Z* conformer of **5b**. Torsion angles α and α' around the C–N bonds of DACH molecules are uniformly negative, in the range –9° to –25°, as expected for the *R*,*R* configuration of the DACH scaffold.

Bis-phthalimide **6** and isothiocyanate-phthalimide **7** derivatives of DACH are conformationally restricted molecules, with little rotational freedom around the C–N bonds. This is apparently due to the steric constraints imposed by the phthalimide group(s). Hence, the only accessible conformers are these with eclipsed H–C_{DACH}–C=O bonds (torsion angles α *ca.* 5°). The isothiocyanate substituent in **7** is turned away from the phthalimide moiety, hence angle α is synclinal (62°).

Phthalimide-thiourea derivatives **8a** and **8b** display structural diversity due to *Z*,*E* conformational changes of the thiourea chromophore. For **8a** three structures of nearly equal calculated energy/population were found, differing in *Z*,*E*, *Z*,*Z* and *E*,*Z* conformation of the thiourea chromophore (Table 1). In the case of **8b**, the analog of **8a** with a more bulky cyclohexyl substituent attached to the thiourea moiety, only two low-energy structures, *Z*,*Z* and *E*,*Z*, were found, the former being the most stable and accounting for 76% of the conformer population (Table 1). This is in agreement with the data for **2b** and **5b** discussed earlier. Torsion angle α H–C_{DACH}–N–C(=S) is positive for all structures of **8a** and **8b** whereas the phthalimide torsion angles α' are negative for *Z*,*E* and *Z*,*Z* structures and positive for the *E*,*Z* structure. A more complex bis-phthalimide-thiourea derivative **9** shows less conformational freedom compared to **8a** and **8b**. The lower-symmetry (C_1) conformer (*E*,*Z*) is the dominant one (94%) in the equilibrium mixture containing also a C_2 symmetry structure (*Z*,*Z*). As in the case of **8a** and **8b**, torsion angles α H–C_{DACH}–N–C(=S) are positive, in the range

32–40°, whereas the phthalimide torsion angles α' are negative (Table 1).

For rigid chiral C_2-symmetric thiourea **10** the only available low-energy structure is of *E*,*E* conformation with the torsion angle α H–C_{DACH}–N–C(=S) –81°. Due to the cyclic *E*,*E* conformation this structure is different from the structures of acyclic thioureas **2b**, **5b**, **8b** and **9**, and therefore is of interest with respect to the chiroptical properties of the thiourea chromophore.

We note that thioureas **5a**, **5b**, **8a**, and **8b** undergo slow (on the NMR timescale) conformational changes, resulting in broadening of the NH signals (see ESI).

Absorption and circular dichroism spectra

Having established the structures of molecules **1–10**, we were able to calculate their electronic spectra (UV and CD) using the TDDFT metod.

In order to test which combination of functional/basis set performs better for calculation of the CD spectra of **1–10**, two different functionals, B3LYP and the double-hybrid functional B2PLYP, recently introduced by Grimme and coworkers, have been employed in combination with 6-311++G(2d,2p) basis set.[27,42] Due to the size of the molecules, we do not perform additional CIS(D) perturbative corrections calculations, thus our results refer to the TD-B2LYP method.[33]

Although each experimental spectrum was reproduced satisfactorily by either B3LYP or B2LYP hybrid functionals in conjunction with the basis sets augmented with diffuse functions, better overall agreement was obtained with the use of the B2LYP hybrid functional combined with 6-311++G(2d,2p) basis set. We note that while B3LYP consistently underestimated the excitation energy, the opposite was observed with the use of the B2LYP functional.

There are five types of chromophores which are included in molecules **1–10**, *i.e.* the isothiocyanate, the *Z*,*E*-, *Z*,*Z*- and *E*,*E*-thiourea, and the phthalimide. In order to determine the nature of the electronic transitions involved in the absorption spectra of these chromophores, the UV spectra of the minimalistic structures **1a**, **2a** (*E*,*Z* and *Z*,*Z*), **3a** and **10′** were calculated using the B2LYP/6-311++G(2d,2p) method. In these structures the cyclohexyl substituents were replaced by the methyl groups and the cyclohexane ring in **10** was removed to leave the chiral structure intact in **10′** (see Chart 1 and Fig. 4).

Fig. 4 shows the calculated electronic transitions of the five chromophores as well as the directions of polarizations of the identified electronic transitions. For methyl isothiocyanate (**1a**) there are two n–π* transitions involving the sulfur atom of the thiocarbonyl group at the longer-wavelength part of the spectrum. The most intensive band, located at *ca.* 200 nm, is presumably of π–π* character and polarized along the S=C=N bond axis (*x*–*y*).

The three thiourea chromophores in molecules **2a**(*E*,*Z*), **2a**(*Z*,*Z*) and **10′**(*E*,*E*) differ in configuration and in the energies and intensities of their electronic transitions. In fact, the shapes of the calculated UV spectra of configurational isomers of **2a** differ significantly (see Fig. E, ESI). A common feature of these chromophores is the presence of a low intensity Rydberg ($n_{(S)}$–RY*) transition in the lowest energy part of the electronic spectrum (*ca.* 280 nm). This transition, polarized along the C=S

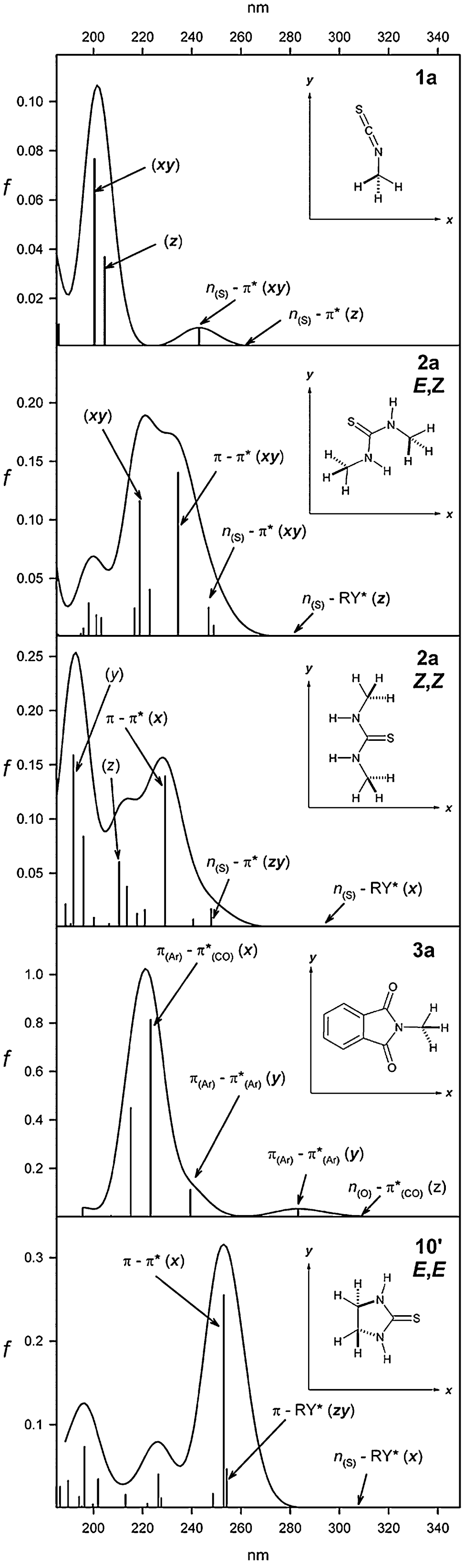

Fig. 4 Calculated at TDDFT/B2LYP/6-311++G(2d,2p) level of theory UV spectra, oscillator strengths (vertical bars) and directions of polarizations of main electronic transitions for model compounds **1a**, **2a**, **3a** and **10′**. All calculated spectra were wavelength-corrected to match the experimental UV spectra of **1b**, **2b**, **3b** and **10** respectively.

bond axis, is insignificant with respect to its contribution to the CD spectra. For the conformers of **2a** low intensity the $n_{(S)}$–π* transition is found in the region at *ca.* 250 nm. The most intense electronic transition is of predominantly the π–π* type in all three configurational isomers of the thiourea chromophore. This transition is located in a 230–235 nm spectral range, polarized along the C=S bond and involves the orbitals of the thiourea molecule. In thiourea molecule of *E*,*E* conformation (molecule **10′**) the π–π* transition is red-shifted to *ca.* 250 nm and is more intense than that found for the *E*,*Z* and *Z*,*Z* isomers.

The electronic transitions of the phthalimide chromophore were studied previously with the use of semiempirical calculations and linear dichroism measurements.[15] The present DFT study of the electronic transitions in *N*-methylphthalimide (**3a**) confirms the presence of a long-wavelength n–π* transition at *ca.* 310 nm and of at least three electronic π–π* transitions below 290 nm, the most intense (π_{Ar}–π^*_{CO}) located at *ca.* 220 nm and polarized along the molecular symmetry axis (Fig. 4).

The experimental and calculated electronic absorption spectra of compounds **1–10** and the electronic CD spectra of compounds **4–10** are shown in Fig. 5 and 6.

The calculated UV spectra are conformation-averaged. For the UV and CD spectra of individual conformers see ESI, Fig. E–M. In general, out of the two functionals used, B3LYP and B2LYP, the latter provides UV and CD spectra with a better match for the experimental spectra. Therefore, further discussion will be limited to the results obtained with the use of the B2LYP functional.

Except **10**, all chiral molecules are bichromophoric or trichromophoric, and one may expect that the CD spectra will be dominated by exciton interactions between the electronically allowed (π–π* type) transitions. Indeed, the shapes of the CD spectra and significant magnitudes of the Cotton effects observed support the exciton origin of the most intense Cotton effects.[43]

Bis-isothiocyanate **4** displays a strong negative Cotton effect (Δε −94) located at 195 nm which is associated with a strong UV

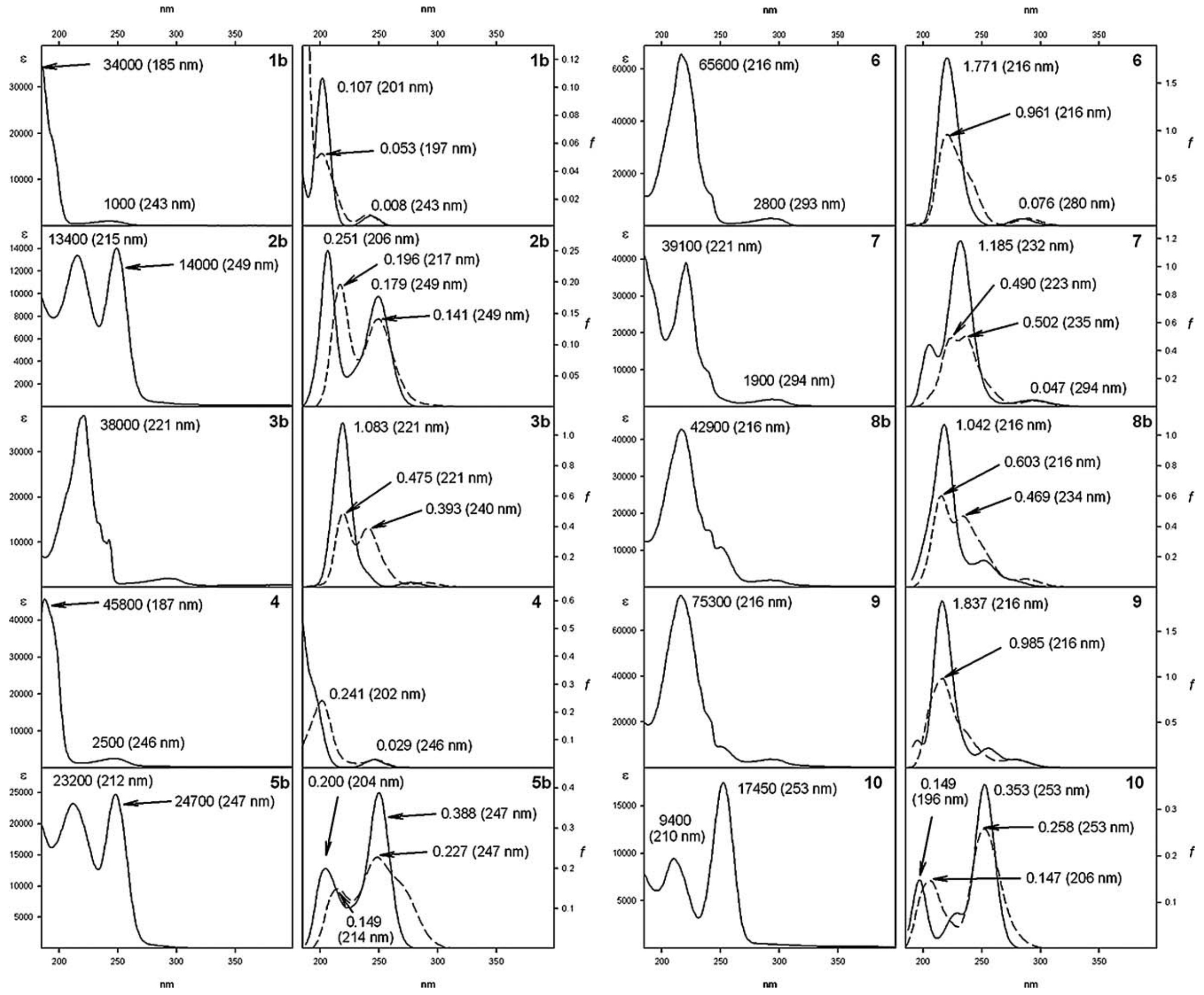

Fig. 5 Experimental (solid lines, left columns) and calculated at B2LYP/6-311++G(2d,2p) (solid lines, right columns) and B3LYP/6-311++G(2d,2p) (dashed lines, right columns) UV spectra for compounds **1–10**. All calculated spectra are scaled in oscillator strength (*f*) and wavelength-corrected to match the experimental UV spectra (see Experimental for details).

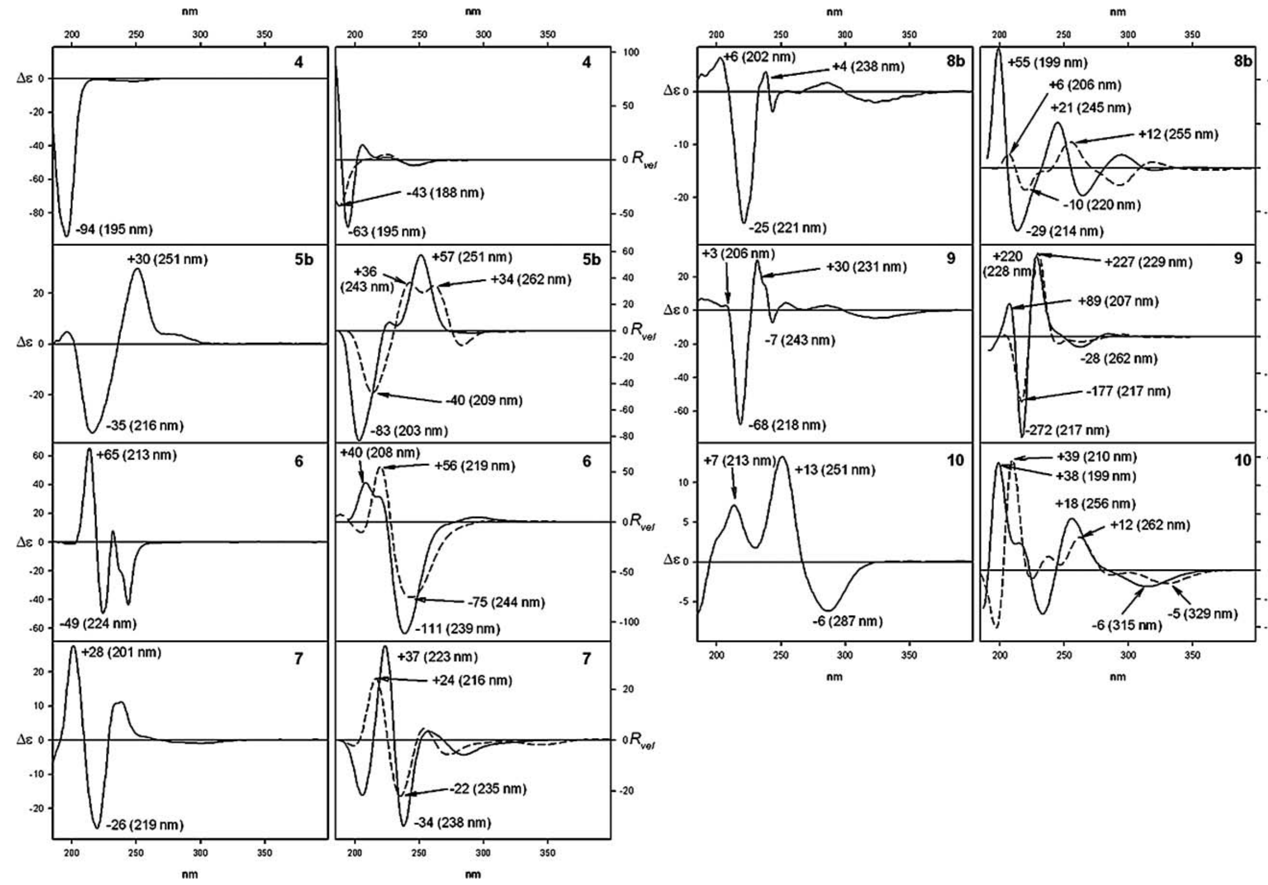

Fig. 6 Experimental (solid lines, left columns) and calculated at B2PLYP/6-311++G(2d,2p) (solid lines, right columns) and B3LYP/6-311++G(2d,2p) levels (dashed lines, right columns) CD spectra for compounds **4–10**. All calculated spectra are scaled in rotatory strength (R_{vel}) and wavelength-corrected as in Fig. 5.

maximum below 190 nm. The calculation shows the presence of a negative exciton couplet ($R = -63$ at 199 nm; +98 at 187 nm) in the CD spectrum of **4**. A negative exciton couplet is obtained for the calculated CD spectra of the most abundant (78% conformer population) family of diequatorial **4***ap*,*sc* conformers (Fig. H, ESI). These results are in full agreement with the model in which the electric dipole transition moments for the π–π* transitions of the two isothiocyanate chromophores form a negative-helicity exciton system.

The experimental UV and CD spectra of **5b** are quite well reproduced by the calculations, especially with the use of B2LYP functional. Both experimental and calculated CD spectra show the presence of a long-wavelength negative Cotton effect just below 300 nm, due to a formally forbidden $n_{(S)}$–π* transition (Fig. 6). The presence of the allowed π–π* transitions in the thiourea chromophore makes possible interpretation of the CD spectrum of bis-thiourea molecule **5b** within the exciton coupling model. The absorption bands of **5b** at 249 nm and 215 nm (Fig. 5) correspond to a positive exciton couplet (Δε +30 at 251 nm, –35 at 216 nm) in the CD spectrum (Fig. 6).

According to calculations, the pattern of signs of the exciton Cotton effects is quite complex and to some extent dependent on the conformation of the thiourea chromophore. Thus, for the most populated *Z*,*Z*,*E*,*E* and *Z*,*Z*,*Z*,*E* stereoisomers of **5b** (Fig. J, ESI) the calculations performed with the B2LYP functional provide the pattern of signs of the most intense Cotton effects (+ at *ca.* 250 nm, – at *ca.* 205 nm) similar to that in the experimental and in calculated, population-weighted CD spectra (Fig. 6). The presence of at least two orthogonal π–π* transitions in each thiourea chromophore (*cf.* Fig. 4) is responsible for a complex pattern of the Cotton effects observed in the calculated CD spectra of structurally related bis-thiourea **5a** (Fig. I, ESI). Nevertheless, the characteristic +/– sequence of the Cotton effects is found in the calculated CD spectra of **5a** and **5b** and also in the experimental CD spectrum of **5b** and can be considered as a diagnostic feature of the bis-thiourea chromophoric system in a *M* helicity arrangement, here imposed by the absolute configuration of (*R*,*R*)-DACH molecule. In addition we note that the experimental CD spectrum of **5a** is very similar to that of **5b** (Fig. N, ESI).

Bis-phthalimide **6** is reported here as a reference molecule, and the analysis of its CD spectrum within the exciton coupling model has been described earlier.[15,17] The DFT calculations reproduce the experimental CD spectrum of **6** quite well with the use of B2LYP functional. This is because molecule **6** is conformationally restricted, having a single energy minimum (shown in Table 1). Since the most intense π–π* phthalimide transition is polarized along its C_2 axis and its direction is rotation-independent, the phthalimide can be used as a reference chromophore of choice for determining the heterochromophoric coupling in derivatives **7–9**.

Whereas the absorption spectra of derivatives of *N*-phthaloyl-1,2-diaminocyclohexane **7–9** are dominated by a strong absorption band at *ca.* 220 nm, the corresponding CD spectra display distinct exciton Cotton effects due to coupling of phthalimide and isothiocyanate transitions in **7** ($\Delta\varepsilon$ −26 at 219 nm, +28 at 201 nm), or phthalimide and thiourea transitions in **8b** ($\Delta\varepsilon$ +4 at 238 nm, −25 at 221 nm) and **9** ($\Delta\varepsilon$ +30 at 231 nm, −65 at 218 nm). These spectral features can also be found in the calculated CD spectra with the use of the B2LYP functional (Fig. 6). Moreover, the experimental CD spectra of **8a** and **8b**, differing in the substitution of the thiourea moiety, are very similar (see Fig. N, ESI). The computed CD spectra for individual conformers of **8a** (Fig. K, ESI) show significant differences, while the CD spectra of individual conformers of **8b** and **9** (Fig. L and M, ESI) all show the characteristic pattern of the exciton Cotton effects, positive at *ca.* 240 nm and negative at *ca.* 220 nm. Note, however, that the results of calculations are sensitive to the functional used, *i.e.* for *E*,*Z* and *Z*,*Z* conformers of **9** consistent results were obtained with the B2LYP functional.

The CD spectrum of monothiourea **10** displays three Cotton effects (Fig. 6). Long-wavelength negative Cotton effect at 287 nm is presumably of $n_{(S)}$–π^* character whereas two positive π–π^* Cotton effects are located at 251 and 213 nm. We note that a positive Cotton effect at 251 nm results from a negative helicity of the thiourea chromophore (negative N–C–C–N torsion angle). This is in accordance with a general helicity rule[44] predicting a positive rotational strength for the transition polarized in a plane perpendicular to the C_2 axis in a chromophore of *M* helicity.

Conclusions

The present study shows that synthetically important thioureas and isothiocyanates can also be considered as chromophores for stereochemical studies by electronic circular dichroism. Despite rotational freedom around the carbon–nitrogen bonds, conformational constraints for model molecules could be determined by the calculations at the DFT B3LYP/6-311++G(2d,2p) level. Whereas a number of low-energy rotamers were found for isothiocyanates **1b** and **4**, the presence of a bulky vicinal phthalimide group in **7** significantly restricted the accessible conformers to just one. Thioureas **2**, **5**, **8** and **9** showed a preference toward *E*,*Z* or *Z*,*Z* conformation, with conformer distribution depending on the substituents at the nitrogen atoms. Low-energy *E*,*E* conformers were not observed for acyclic thioureas. TDDFT calculations at B2LYP/6-311++G(2d,2p) level provided UV and CD spectra in very good agreement with the experimental data. These results could be rationalized within the exciton coupling model for the allowed π–π^* transitions. The main transitions of high oscillator strengths which are responsible for the appearance of exciton Cotton effects in the CD spectra are polarized along the N=C=S bond system in isothiocyanates (*ca.* 190 nm) along the C=S bond axis (240–250 nm) and parallel to the N···N direction (*ca.* 210 nm) in thioureas. Using the phthalimide as an external reference chromophore, whose most intensive transition (*ca.* 220 nm) is polarized along the chromophore symmetry axis, a simple pattern of exciton Cotton effects in the range 250 to 185 nm can be envisaged, on the basis of the experimental and calculated data (Fig. 7).

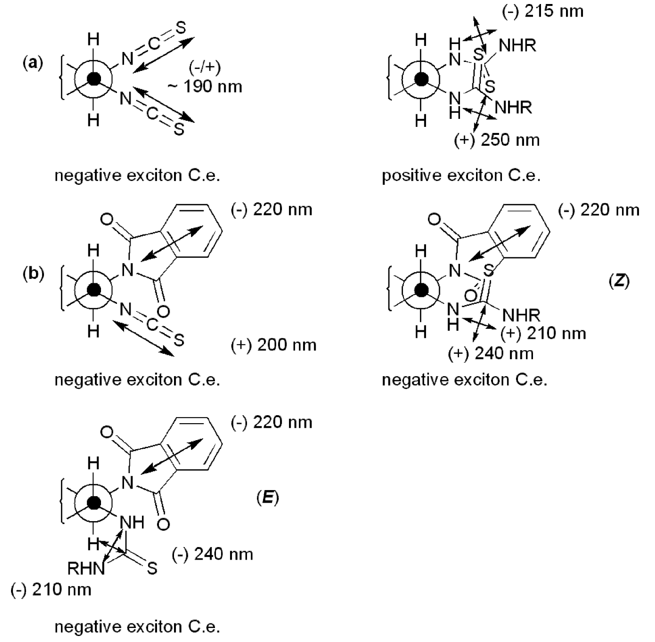

Fig. 7 Pattern of diagnostic exciton Cotton effects due to (**a**) homochromophoric or (**b**) heterochromophoric coupling.

Whereas most of the features of the CD spectra in Fig. 7 are self-explanatory, the complexity of the CD spectra of thioureas merits a few comments. We note that their CD spectra are dependent on the thiourea conformation at the point of attachment to the chiral center (here DACH molecule). Thus, opposite-sign exciton Cotton effects are calculated for *Z* and *E* conformers of **8a** and **8b**, the experimental spectra being dominated by the contribution of *Z* conformers. On the other hand, the exciton Cotton effects of **9** are due to a dominant *E*,*Z* conformer and further sensitive to the contribution due to homochromophoric exciton coupling of the two phthalimide groups.

We anticipate that the results presented here will be useful for structural studies of chiral molecules containing the thiourea or isothiocyanate chromophores (homochromophoric coupling) or in combination of these with other CD active groups (heterochromophoric coupling). Another important finding of the present study is the observation that the B2LYP functional, recently introduced by Grimme *et al.*,[27,42] performs much better than the commonly used B3LYP functional for the calculation of CD spectra. It is recommended that the former be used for the calculations of chiroptical data in a short-wavelength UV absorption region.

Experimental

General

NMR spectra were recorded in deuteriochloroform on a Varian XL300 instrument and are reported in ppm with respect to TMS as a reference. FAB MS were measured with a 604 AMD Intectra spectrometer. FT-IR spectra were taken in KBr pellets with a Bruker IFS 113v spectrometer. CD and UV spectra were measured with a Jasco J-910 spectropolarimeter. Melting points are uncorrected.

Computational methods

In our computations all excited-state calculations have been performed, based upon the ground-state geometries of single molecules, with the use of a Gaussian program package.[30] Optimization of structures were performed using tight convergence criteria. Rotatory strengths were calculated using both length and velocity representations. In the present study the differences between the values of rotatory strengths calculated in length and velocity representations were quite small, and for this reason only velocity representations were taken into account. The computed oscillator strengths and rotational strengths were converted to the UV and CD spectra by broadening to Gaussian-shape absorption curves, according to the procedure described by Grimme *et al.*[45] The calculated spectra were either blue- or red-shifted by *ca.* 10–20 nm in relation to the experimental data, depending on the method used. For scaling the calculated spectra of **3b**, **6**, **8b** and **9** the position of the most intense phthalimide absorption band at *ca.* 220 nm was taken as a reference; in the remaining cases the position of the longest-wavelength absorption band served the purpose. The scaling factors were either smaller or greater than one, depending on the applied either blue or red shift.

Synthesis

5a. To a stirred solution of *trans*-(1*R*,2*R*)-diaminocyclohexane (114 mg, 1 mmol) in dichloromethane (4 mL), methyl isothiocyanate (160 mg, 2.2 mmol) in 2 mL dichloromethane was slowly added *via* syringe. The solution was stirred at room temperature for 5 h. Next the mixture was evaporated to dryness. The crude product was purified by flash chromatography (eluent: 3% MeOH–CH_2Cl_2) to give 109 mg (42% yield) of viscous oil; ^{1}H NMR ($CDCl_3$) δ 1.36 (4H, bs), 1.79 (2H, bs), 2.28 (2H, bs), 2.96–3.03 (6H, m), 4.27 (2H, bs), 6.76 (2H, bs), 7.22 (2H, bs); ^{13}C NMR ($CDCl_3$) δ 15.3, 21.3, 22.2, 22.5, 25.2, 31.5, 34.4, 45.2, 50.1, 73.8, 127.7, 129.7, 135.2, 135.6; IR (KBr) ν/cm^{-1}: 3247, 3064, 2934, 2855, 2215, 1565, 1511, 1500, 1468, 1386, 1343, 1263, 1233, 1178, 1108, 1035, 950, 914, 867, 849, 764, 730, 645; FAB MS (*m/z*) [M$^+$+1] = 261,1; CD (acetonitrile) $\Delta\varepsilon$ (nm): 21.7 (247), −21.2 (212); UV (acetonitrile) ε (nm): 18600 (245), 17400 (210).

5b. To a stirred solution of *trans*-(1*R*,2*R*)-diaminocyclohexane (114 mg, 1 mmol) in dichloromethane (4 mL), cyclohexyl isothiocyanate (311 mg, 0.301 mL, 2.2 mmol) was slowly added *via* syringe. The solution was stirred at room temperature for 5 h. Next the mixture was filtered to remove the precipitate and the filtrate was evaporated to dryness. The crude product was crystallized from benzene to give 268 mg (67% yield) of white crystals; mp 219–223 °C; ^{1}H NMR ($CDCl_3$) δ 1.16–1.97 (26H, m), 2.30 (2H, bs), 3.76 (2H, bs), 4.31 (2H, bs), 5.95 (2H, bs), 6.75 (2H, bs); ^{13}C NMR ($CDCl_3$) δ 24.6, 25.3, 32.4, 32.7, 33.0, 42.6 (bs), 52.3 (bs), 60.2 (bs), 128.3, 179.6 (bs); IR (KBr) ν/cm^{-1}: 3233, 3057, 2929, 2853, 1561, 1549, 1510, 1448, 1335, 1284, 1229, 1083, 980, 944, 888, 867,848, 771, 737, 666, 631, 585; EI MS (*m/z*) [M$^+$] = 396.3; CD (acetonitrile) $\Delta\varepsilon$ (nm): 3.8 (278), 29.8 (251), −35.2 (216), 4.8 (196); UV (acetonitrile) ε (nm): 24700 (248), 23200 (212).

7. To a stirred solution of *trans*-*N*-phthaloyl-(1*R*,2*R*)-diaminocyclohexane[36] (122 mg, 0.5 mmol) in dichloromethane (2 mL), thiophosgene (58 mg, 0.04 mL, 0.6 mmol) was added in one portion *via* syringe. After 10 min of stirring triethylamine (0.14 mL, 101 mg, 1 mmol) was added in one portion. The whole mixture was stirred at room temperature for additional 4 h. Next dichloromethane (2 mL) and water (5 mL) were added to the mixture. The layers were separated, the organic layer was washed with 1 N HCl (2 × 5 mL), dried over magnesium sulfate and evaporated to dryness. The crude product was purified by flash chromatography on silica gel to give 115 mg of white solid which was crystallized from diethyl ether–hexane. Yield after crystallization 89 mg, (63%), mp 77–80 °C; ^{1}H NMR ($CDCl_3$) δ 1.36–1.41 (2H, m), 1.56–1.69 (1H, m), 1.82–1.86 (3H, m), 2.09–2.32 (2H, m), 4.12–4.21 (1H, m), 4.48–4.57 (1H, m), 7.73–7.77 (2H, m), 7.84–7.7.89 (2H, m); ^{13}C NMR ($CDCl_3$) δ 23.9, 24.8, 28.9, 33.6, 54.8, 56.9, 76.6, 123.4, 131.6, 134.2, 168.0; IR (KBr) ν/cm^{-1}: 3460, 2963, 2940, 2866, 2207, 2173, 2080, 1774, 1760, 1718, 1706, 1610, 1466, 1456, 1369, 1372, 1352, 1104, 1067, 1046, 1020, 1002, 952, 931, 901, 867, 837, 789, 711, 635, 528, 466; EI MS (*m/z*) [M$^+$] = 286.1; CD (acetonitrile) $\Delta\varepsilon$ (nm): −1.0 (300), 11.1 (238), −25.9 (219), 27.6 (201); UV (acetonitrile) ε (nm): 1900 (294), 10200sh (236), 39100 (220).

8a. To a stirred solution of *trans*-*N*-phthaloyl-(1*R*,2*R*)-diaminocyclohexane (122 mg, 0.5 mmol) in dichloromethane (2 mL), methyl isothiocyanate (44 mg, 0.6 mmol) in 2 mL of dichloromethane was added in one portion. The mixture was stirred at room temperature overnight. After evaporation to dryness the crude product was purified by chromatography (eluent: 3% MeOH–CH_2Cl_2) to give 95 mg (60% yield) of viscous oil; ^{1}H NMR ($CDCl_3$) δ 1.22–1.64 (3H, m), 1.81–1.92 (3H, m), 2.30–2.34 (1H, bs), 2.47 (1H, bs), 2.81–2.83 (3H, s), 3.97–4.06 (1H, m), 4.66 (1H, bs) 5.60 (1H, bs), 5.84 (1H, bs) 7.70–7.74 (2H, m), 7.80–7.84 (2H, m); ^{13}C NMR ($CDCl_3$) δ 24.5, 25.0, 28.9, 30.6, 33.4, 54.8, 123.3, 131.6, 134.1, 152.1, 169.0, 182.1; IR (KBr) ν/cm^{-1}: 3455, 3357, 3309, 3110, 2934, 2656, 1767, 1700, 1613, 1573, 1539, 1402, 1372, 1284, 1257, 1107, 1068, 1034, 869, 724, 580, 530; FAB MS (*m/z*) [M$^+$+1] = 318.1; CD (acetonitrile) $\Delta\varepsilon$ (nm): −1.6 (324), 2.1 (282), −1.0 (243), 9.2 (236), −28.0 (211), 8.5 (204); UV (acetonitrile) ε (nm): 2050 (292), 11100sh (250), 15790sh (240), 41430 (217).

8b. To a stirred solution of *trans*-*N*-phthaloyl-(1*R*,2*R*)-diaminocyclohexane (122 mg, 0.5 mmol) in dichloromethane (2 mL), cyclohexyl isothiocyanate (85 mg, 0.08 mL, 0.6 mmol) was added in one portion. The mixture was stirred at room temperature overnight and then was heated to reflux for an additional hour. After evaporation to dryness the crude product was crystallized from chloroform–hexane; mp 196–200 °C; ^{1}H NMR ($CDCl_3$) δ 0.99–1.71 (12H, m), 1.82–1.91 (4H, m), 2.32 (1H, bs), 2.40 (1H, bs), 3.64 (1H, bs), 4.03 (1H, t, J = 12.4 Hz), 4.61 (1H, bs) 5.49 (1H, bs), 5.64 (1H, d, J = 8.0 Hz) 7.70–7.74 (2H, m), 7.80–7.82 (2H, m); ^{13}C NMR ($CDCl_3$) δ 24.6, 24.7, 25.3, 29.0, 32.4, 32.7, 33.5, 53.0, 54.9, 76.6, 123.3, 131.7, 134.1, 169.0, 179.9; IR (KBr) ν/cm^{-1}: 3451, 3346, 32,81 3095, 2934, 2920, 2854, 2664, 1762, 1696, 1610, 1567, 1466, 1452, 1395,1320, 1238, 1152, 1132, 1085, 1067, 1017, 1000, 953, 870, 842, 739, 719, 639, 584, 530, 419; EI MS (*m/z*) [M$^+$] = 385.2; CD (acetonitrile) $\Delta\varepsilon$ (nm): −2.1 (323), 1.7 (286), −0.3 (264), 0.1 (255), −3.8 (243), 3.8 (238), −24.9 (221), 6.4 (202); UV (acetonitrile) ε (nm): 1900 (292), 10800 (250), 15400sh (239), 42900 (216).

9. To a stirred solution of *trans*-*N*-phthaloyl-(1*R*,2*R*)-diaminocyclohexane (73 mg, 0.3 mmol) in dichloromethane (2 mL), compound **7** (86 mg, 0.3 mmol) was added in one portion. The mixture was stirred at room temperature overnight. After evaporation of the solvent the crude product was crystallized from methanol to give 64 mg (37% yield) of white crystals; mp 258–260 °C; ^{1}H NMR (CDCl$_3$) δ 1.04–1.13 (2H, m), 1.21–1.46 (4H, m), 1.66–1.78 (2H, m), 1.82–1.86 (4H, m), 2.03 (2H, d, $J = 11.5$ Hz), 2.46–2.53 (2H, m), 3.86–3.95 (2H, m), 4.63 (2H, d, $J = 9.0$ Hz), 5.43 (2H, d, $J = 9.0$ Hz), 7.66 (4H, m); ^{13}C NMR (CDCl$_3$) δ 24.3, 25.3, 28.7, 29.9, 32.9, 54.5, 123.1, 131.8, 133.7, 168.7, 181.7; IR (KBr) ν/cm^{-1}: 1773, 1714, 1706, 1612, 1553, 1514, 1468, 1420, 1391, 1373 1257, 1226, 1164, 1118, 1067, 1015, 724, 713, 637, 530, 482; EI MS (m/z) [M$^+$] = 530.2; CD (acetonitrile) $\Delta\varepsilon$ (nm): −4.7 (323), 2.9 (286), 4.4 (253), −7.3 (243), 30.1 (231), −67.9 (218), 3.0 (207), 6.2 (193); UV (acetonitrile) ε (nm): 292 (3600), 9100 (250), 22500sh (239), 75300 (216).

10. To a stirred solution of *trans*-(1*R*,2*R*)-diaminocyclohexane (57 mg, 0.5 mmol) in dichloromethane (2 mL) thiophosgene (57 mg, 0.5 mmol, 0.2 ml of 2.5 M soln. in dichloromethane) was added slowly *via* syringe. After 10 min of stirring, triethylamine (121 mg, 0.167 mL, 1.2 mmol) was added in one portion and the mixture was stirred at room temperature for 2 h. Next dichloromethane (2 mL) and water (3 mL) were added to the mixture. The layers were separated, the organic layer was washed with 1 N HCl (2 × 3 mL), dried over magnesium sulfate and evaporated to dryness. The crude product was purified by flash chromatography on silica gel to give white solid (54 mg, 69% yield); mp 168–171, 203–205 °C (lit.[46] for *rac*-**10**, mp 148–150 °C); ^{1}H NMR (CDCl$_3$) δ 1.29–1.60 (4H, m), 1.78–1.86 (2H, m), 2.04–2.08 (2H, m), 3.28–3.33 (2H, m) 6.34 (2H, bs); ^{13}C NMR (CDCl$_3$) δ 23.8, 28.9, 64.8, 187.8; IR (KBr) cm-1 3210, 2953, 2933, 2663, 1506, 1457, 1353, 1304, 1254, 1219, 1171, 1139, 1102, 943, 924, 830, 702, 651, 620, 596, 484, 426; EI MS (m/z) [M$^+$] = 156.2; CD (acetonitrile) $\Delta\varepsilon$ (nm): −6.2 (286), 13.3 (251), 7.1 (213); UV (acetonitrile) ε (nm): 17450 (252), 9400 (210).

Acknowledgements

This work was supported by a grant no. PBZ-KBN-126/T09/10 from the Ministry of Science. All calculations have been performed at the Poznań Supercomputing and Networking Centre, Poland.

References

1 A. A. Aly, E. K. Ahmed, K. M. El-Mokadem and M. E.-A. F. Hegazy, *J. Sulfur Chem.*, 2007, **28**, 73–93.

2 M. Koketsu and H. Ishihara, *Curr. Org. Synth.*, 2006, **3**, 439–455.

3 E. Rodriguez-Fernández, J. L. Manzano, J. J. Benito, R. Hermosa, E. Monte and J. J. Criado, *J. Inorg. Biochem.*, 2005, **99**, 1558–1572.

4 R. Custelcean, *Chem. Commun.*, 2008, 295–307.

5 S. Connon, *Chem. Commun.*, 2008, 2499–2510.

6 X. Yu and W. Wang, *Chem. Asian J.*, 2008, **3**, 516–532.

7 A. G. Doyle and E. N. Jacobsen, *Chem. Rev.*, 2007, **107**, 5713–5743.

8 J. L. Vicario, D. Badia and L. Carrillo, *Synthesis*, 2007, 2065–2092.

9 Q.-H. Wu, Y.-J. Gao, Z. Li, J.-M. Wang, C. Wang, J.-J. Ma and S.-J. Song, *Chinese J. Org. Chem.*, 2007, **27**, 1491–1501.

10 T. Akiyama, J. Itoh and K. Fuchibe, *Adv. Synth. Catal.*, 2006, **348**, 999–1010.

11 A. Berkessel and H. Gröger, *Asymmetric Organocatalysis*, Wiley-VCh, Weinheim, 2005, Chapter 5.

12 C. Palomo, M. Oiarbide and A. Mielgo, *Angew. Chem. Int. Ed.*, 2004, **43**, 5442–5444.

13 F. Wu, Z. Wen and Y. Jiang, Y., *Progress, in Chemistry*, 2004, **16**, 776–784.

14 L. Ilisz, R. Berkecz and A. Péter, *J. Pharm. Biomed. Anal.*, 2008, **47**, 1–15.

15 J. Gawronski, F. Kazmierczak, K. Gawronska, U. Rychlewska, B. Nordén and A. Holmén, *J. Am. Chem. Soc.*, 1998, **120**, 12083–12091.

16 J. Gawronski, K. Gawronska, P. Skowronek and A. Holmén, *J. Org. Chem.*, 1999, **64**, 234–241.

17 J. Gawronski, M. Brzostowska, K. Kacprzak, H. Kołbon and P. Skowronek, *Chirality*, 2000, **12**, 263–268.

18 J. Gawronski and P. Skowronek, *Curr. Org. Chem.*, 2004, **8**, 65–82.

19 (*a*) T. Helgaker, T. A. Ruden, P. Jørgensen, J. Olsen and W. Klopper, *J. Phys. Org. Chem.*, 2004, **17**, 913; (*b*) V. Barone, R. Improta and N. Rega, *Acc. Chem. Res.*, 2008, **41**, 605–616.

20 M. F. C. Ladd and R. A. Palmer, *Structure Determination by X-ray Crystallography*, 2nd edn, Plenum Press, New York, 1985.

21 see for example: B. C. Rinderspacher and P. R. Schreiner, *J. Phys. Chem. A*, 2004, **108**, 2867–2870.

22 (*a*) T. D. Crawford, *Theor. Chem. Acc.*, 2006, **115**, 227–245; (*b*) T. D. Crawford and P. J. Stephens, *J. Phys. Chem. A*, 2008, **112**, 1339–1345; (*c*) T. D. Crawford, M. C. Tam and M. L. Abrams, *J. Phys. Chem. A*, 2007, **111**, 12057–12068 and literature cited therein.

23 K. Burke, J. Werschnik and E. K. U. Gross, *J. Chem. Phys.*, 2005, **123**, 062206.

24 (*a*) J. Tirado-Rives and W. L. Jorgensen, *J. Chem. Theory Comput*, 2008, **4**, 297–306; (*b*) Y. Zhao and D. G. Truhlar, *Acc. Chem. Res.*, 2008, **41**, 157–167.

25 (*a*) P. R. Schreiner, *Angew. Chem. Int. Ed*, 2007, **46**, 4217–4219; (*b*) M. D. Wodrich, C. Corminboeuf, P. R. Schreiner, A. A. Fokin and P. van Ragu Schleyer, *Org. Lett*, 2007, **9**, 1851–1854; (*c*) P. R. Schreiner, A. A. Fokin, R. A. Pascal and A. de Meijere, *Org. Lett*, 2006, **8**, 3635–3638; (*d*) Y. Zhao and D. G. Truhlar, *Org. Lett*, 2006, **8**, 5753–5755; (*e*) C. E. Check and T. M. Gilbert, *J. Org. Chem.*, 2005, **70**, 9828–9834.

26 (*a*) R. J. Bartlett, V. F. Lotrich and I. V. Schweigert, *J. Chem. Phys*, 2005, **123**, 062205; (*b*) P. Mori-Sánchez, Q. Wu and W. Yang, *J. Chem. Phys.*, 2005, **123**, 062204; (*c*) E. J. Baerends and O. V. Gritsenko, *J. Chem. Phys.*, 2005, **123**, 062202; (*d*) A. Görling, *J. Chem. Phys*, 2005, **123**, 062203 and literature cited therein.

27 S. Grimme, *J. Chem. Phys*, 2006, **124**, 034108.

28 F. Neese, T. Schwabe and S. Grimme, *J. Chem. Phys.*, 2007, **126**, 124115.

29 R. Ahlichrs, M. Bär, M. Häser, H. Horn and C. Kölmel, *Chem. Phys. Lett.*, 1989, **162**, 165–169 (see also www.turbomole-gmbh.com for an overview of the TURBOMOLE program).

30 M. J. Frisch, G. W. Trucks, H. B. Schlegel, G. E. Scuseria, M. A. Robb, J. R. Cheeseman, V. G. Zakrzewski, J. A. Montgomery, Jr., R. E. Stratmann, J. C. Burant, S. Dapprich, J. M. Millam, A. D. Daniels, K. N. Kudin, M. C. Strain, O. Farkas, J. Tomasi, V. Barone, M. Cossi, R. Cammi, B. Mennucci, C. Pomelli, C. Adamo, S. Clifford, J. Ochterski, G. A. Petersson, P. Y. Ayala, Q. Cui, K. Morokuma, P. Salvador, J. J. Dannenberg, D. K. Malick, A. D. Rabuck, K. Raghavachari, J. B. Foresman, J. Cioslowski, J. V. Ortiz, A. G. Baboul, B. B. Stefanov, G. Liu, A. Liashenko, P. Piskorz, I. Komaromi, R. Gomperts, R. L. Martin, D. J. Fox, T. Keith, M. A. Al-Laham, C. Y. Peng, A. Nanayakkara, M. Challacombe, P. M. W. Gill, B. Johnson, W. Chen, M. W. Wong, J. L. Andres, C. Gonzalez, M. Head-Gordon, E. S. Replogle and J. A. Pople, *Gaussian 03*, Gaussian, Inc., Pittsburgh PA, 2001.

31 S. Grimme and F. Neese, *J. Chem. Phys.*, 2007, **127**, 154116.

32 M. Head-Gordon, R. J. Rico, M. Oumi and T. J. Lee, *Chem. Phys. Lett.*, 1994, **219**, 21–29.

33 L. Goerigk and S. Grimme, *J. Phys. Chem. A*, 2009, **113**, 767–776.

34 G. González, N. Yutronic and M. Jara, *Spectrochim. Acta*, 1990, **46A**, 1729–1736.

35 E. J. Crust, I. J. Munslow and P. Scott, *J. Organomet. Chem.*, 2005, **690**, 3373–3382.

36 M. Kaik and J. Gawronski, *Tetrahedron: Asymmetry*, 2003, **14**, 1559–1563.

37 L. V. Sudha and D. N. Sathyanarayana, *Spectrochim. Acta*, 1984, **40A**, 751–755.

38 (*a*) R. H. Sullivan, P. Nix, E. L. Summers and S. L. Parker, *Org. Magn. Reson.*, 1983, **21**, 293–300; (*b*) R. H. Sullivan and E. Price, *Org. Magn. Reson.*, 1975, **7**, 143–150.
39 (*a*) A. Ramnathan, K. Sivakumar, K. Subramanian, D. Meerarani, K. Ramadas and H.-K. Fun, *Acta Cryst.*, 1996, **C52**, 139–142; (*b*) A. Ramnathan, K. Sivakumar and K. Subramanian, *Acta Cryst.*, 1995, **C51**, 2446–2450.
40 R. K. Gosavi, U. Argawala and C. N. R. Rao, *J. Am. Chem. Soc.*, 1967, **89**, 235–239.
41 R. Custelcean, M. G. Gorbunova and P. V. Bonnesen, *Chem. Eur. J.*, 2005, **11**, 1459–1466.
42 (*a*) T. Schwabe and S. Grimme, *Phys. Chem. Chem. Phys.*, 2007, **9**, 3397; (*b*) S. Grimme, J. Antony, T. Schwabe and C. Mück-Lichtenfeld, *Org. Biomol. Chem.*, 2007, **5**, 741–758.
43 For a comparison of quantum chemical methods for investigation of exciton coupling, see: Goerigk and S. Grimme, *ChemPhysChem*, 2008, **9**, 2467–2470.
44 W. Hug and G. Wagniere, *Tetrahedron*, 1972, **28**, 1241–1248.
45 C. Diedrich and S. Grimme, *J. Phys. Chem. A*, 2003, **107**, 2524–2539.
46 S. G. Davies and A. A. Mortlock, *Tetrahedron*, 1993, **49**, 4419–4438.